

QUANTUM DYNAMICS OF JAHN-TELLER COMPLEXES $\text{Cr}^{2+}\text{F}_8^-$ IN A $\text{CdF}_2 : \text{Cr}$ CRYSTAL

© 2024 M.N. Sarychev^a, N. Yu. Ofitserova^a, I. V. Zhevstovskikh^{a,b}, A. V. Egranov^{c,d}, V. T. Surikov^e, N. S. Averkiev^f, V. V. Gudkov^{a,*}

^aUral Federal University, Ekaterinburg 620002, Russia

^bMikheev Institute of Metal Physics, Ural Branch of Russian Academy of Sciences, Ekaterinburg, 620137, Russia

^cVinogradov Institute of Geochemistry, Siberian Branch of Russian Academy of Sciences, Irkutsk 664033, Russia

^dIrkutsk State University, Irkutsk 664003, Russia

^eInstitute of Solid State Chemistry, Ural Branch of Russian Academy of Sciences, Ekaterinburg 620990, Russia

^fIoffe Institute, St.-Petersburg 194021, Russia

*e-mail: v.v.gudkov@urfu.ru

Received September 10, 2023

Revised September 30, 2023

Accepted October 02, 2023

Abstract. The results of ultrasonic studies of a crystal with a fluorite structure CdF_2 doped with low concentration chromium atoms ($n_{\text{Cr}} = 6.3 \cdot 10^{19} \text{ cm}^{-3}$ with a predominance of Cr^{3+} ions) were presented. The measurements were performed in the range of 3.6–150 K at frequencies 18–268 MHz using transverse and longitudinal normal modes propagating in the crystallographic direction [100]. The anomalies characteristic for systems of Jahn-Teller cubic complexes with orthorhombic minima of the adiabatic potential have been discovered in the temperature dependence of the attenuation and velocity of ultrasonic waves. The interpretation of the results was carried out in the framework of the quadratic $T \otimes (e + t_2)$ problem of the Jahn-Teller effect for $\text{Cr}^{2+}\text{F}_8^-$ complexes, whose concentration was of the order of $10^{-2} n_{\text{Cr}}$. The analysis of the experimental data made it possible to determine the configurational relaxation mechanisms of the Jahn-Teller subsystem and the values of the parameters that determine them.

Keywords: Jahn-Teller effect, vibronic interaction, doped crystals, semiconductors, quantum tunneling, potential barrier, relaxation, elastic moduli, ultrasonic waves

DOI: 10.31857/S00444510240208e6

1. INTRODUCTION

Crystals doped with transition metal ions have attracted increased attention in terms of fundamental research and in connection with their practical applications in laser devices, electronics and quantum computing [1–3]. The alloying impurities of the same chemical element, but in different charge states, show different properties. The alloying impurities of the same chemical element, but in different charge states, show different properties. As an example, crystals with fluorite structure (space group $Fm\bar{3}m$, Fig. 1) in which chromium impurities appear in Cr^+ , Cr^{2+} and Cr^{3+} states [4–6]. In this connection, the question arises about the methods of their studies, which would be focused on ions with a certain charge state in particular, when the ions of one state are the dominant, and

other ones are small additive. The unique opportunity to realize this program is provided by physical acoustics methods in the presence of ions forming Jahn-Teller (JT) complexes. A unique opportunity for the implementation of this program is provided by physical acoustics methods in the presence of ions forming Jahn-Teller (JT) complexes. In particular, the ground state 5D of the free Cr^{2+} ion (d^4) in a crystal field of cubic (or tetrahedral) symmetry splits into an orbital doublet 5E (excited state) and an orbital triplet 5T_2 (ground state) [7]. Since both of these states are degenerate, further consideration requires taking into account the Jahn-Teller effect (JTE) (see, e.g., [8]).

Due to the smallness of the phonon energy used in the ultrasonic experiment, it is extremely difficult to observe resonance transitions between vibronic levels. This is easily understood if we estimate the phonon

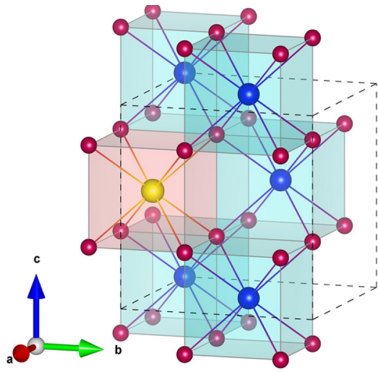


Fig. 1. Structure of isovalent substituted $\text{CdF}_2 : 3d$ crystal. The $3d$ ion (yellow color), in this work Cr^{2+} , substitutes Cd^{2+} and, surrounded by eight fluorine ions (red positions), and forms a cubic JT complex.

energy used in the experiment. Thus, at a frequency of 100 MHz in temperature units it is ≈ 5 mK. That is, only at very low temperatures transitions between closely spaced levels in the form of resonance-type anomalies can manifest themselves. Thus, changes from the external parameter of dispersion and absorption curves of ultrasonic wave can have only relaxation nature. This fact was established in the very first works on the study of JTE in doped crystals by ultrasonic methods (see review [9]).

The nonequilibrium introduced by the ultrasonic wave into the JT subsystem leads to redistribution of JT complexes by strain-dependent energy levels, and the mechanisms leading to the equilibrium state at low temperatures are quantum in nature. In this connection, it makes sense to call the relaxation time of the energy distribution function of complexes of different configurations configurational (Jahn-Teller, vibronic) to distinguish it from the spin-spin or spin-lattice relaxation time, and the low-temperature dynamics of complexes is quantum in contrast to that observed at higher temperatures [10, 11].

In doped crystals with fluorite structure, anomalies of relaxation nature were found in $\text{SrF}_2:\text{Cr}^{2+}$ [12], $\text{CaF}_2:\text{Ni}^{2+}$ [13], $\text{CaF}_2:\text{Cr}^{2+}$ [14], and $\text{CaF}_2:\text{Cu}^{2+}$ [15]. Ultrasonic experiments performed in all the above crystals have shown that the global minima of the adiabatic potential (AP) of JT-complexes have orthorhombic symmetry, which is possible only in the case of a quadratic $T \otimes (e + t_2)$ JTE problem or due to lattice anharmonicity (see, e.g., [16]). In this case, the reasons for the formation of orthorhombic AP global minima are certainly interesting, but not important for the interpretation of the experimental data. Where

they could be compared with the JTE data regarding the symmetry properties of the environment, they always coincided under the assumption of isovalent substitution of the cation by the JT ion [5, 17, 18].

In the previously studied CaF_2 and SrF_2 crystals with chromium ion substitution of cations, an increase in the mass of the metal atom in the MeF_2 matrix led to an increase in the activation energy and, consequently, an increase in the potential barrier height and the low-temperature value of the relaxation time. Since the activation energy was quite large in the SrF_2 matrix, 264 cm^{-1} , compared to 91.7 cm^{-1} for the CaF_2 matrix, it was of interest to establish whether this trend would continue for the heavier cation? The present work therefore focuses on the study of the $\text{CdF}_2 : \text{Cr}$ crystal and comparing the data with those previously obtained for other crystals with fluorite structure.

2. EXPERIMENT

The samples used in this work were cut from the original $\text{CdF}_2 : \text{Cr}$ and CdF_2 crystals shown in Fig. 2. They were grown in the A.P. Vinogradov Institute of Geochemistry, Siberian Branch of Russian Academy of Sciences by the Bridgman-Stockbarger method in a graphite crucible in an inert atmosphere. CrF_3 , vacuum dried, was used as an activator. The composition of the doped crystal was analyzed using ELAN 9000 ICP-MS (Perkin-Elmer SCIEX) at the Institute of Solid State Chemistry, Ural Branch of the Russian Academy of Sciences. The concentration of chromium impurity was $n_{\text{Cr}} = (6.29 \pm 0.03) \cdot 10^{19} \text{ cm}^{-3}$. The concentrations of transition metals capable of forming threefold degenerate states of ions in the cubic environment, Mn^{3+} and V^{2+} , were an order of magnitude smaller, and Ni^{2+} and Cu^{2+} were two orders of magnitude smaller than n_{Cr} .

Ultrasonic measurements were carried out at the Institute of Physics and Technology of Ural Federal University using an installation operating on the principle of a frequency-tunable high-frequency bridge [19]. Resonant piezoelectric transducers made of lithium niobate were used for generation and registration of ultrasonic oscillations. The measurement errors of absorption and phase velocity changes were 0.1 dB and 10^{-5} , respectively. Measurements of the temperature dependences of the absorption coefficient $\alpha = -\text{Im}k$ and phase velocity $v = \omega / \text{Re}k$, where $k = \text{Re}k - i\alpha$ is the complex wave number, were performed in the interval $T = 3.6\text{--}150$ K at frequencies $\omega/2\pi = 18\text{--}268$ MHz. The measurement results can be presented in the form of temperature dependences $\Delta\alpha_\beta / k_0$ and $\Delta v_\beta / v_0$ or $\text{Im}\Delta c_\beta / c_0$ and $\text{Re}\Delta c_\beta / c_0$. At small changes in the values

$$\frac{\text{Re} \Delta c_\beta}{c_0} = 2 \frac{\Delta v_\beta}{v_0}, \quad (1)$$

$$\frac{\text{Im} \Delta c_\beta}{c_0} = 2 \frac{\Delta \alpha_\beta}{k_0}, \quad (2)$$

where the index β characterizes the type of normal mode and the corresponding component of the dynamic elastic modulus tensor \mathbf{c} , and the index 0 denotes the value determined at some fixed value of temperature T_0 .

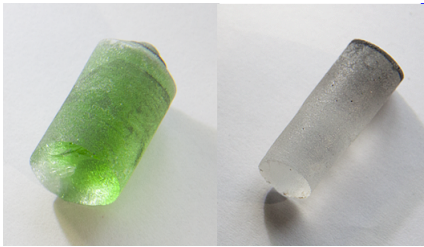


Fig. 2. Crystals of $\text{CdF}_2 : \text{Cr}$ (left) and nominally pure CdF_2 (right).

The elastic moduli tensor of a crystal is the sum of contributions of various subsystems, including the subsystem formed by the JT-complexes. The JT contribution to the components of the dynamic elastic moduli tensor has the following form (see, for example, [15])

$$\frac{c_\beta^{JT}}{c_0} = \frac{(c_\beta^{JT})^T}{c_0} \frac{1}{1 + i\omega\tau} = \frac{(c_\beta^{JT})^T}{c_0} (f_1 - if_2), \quad (3)$$

where $(c_\beta^{JT})^T$ – contribution of the JT subsystem to the isothermal modulus of elasticity, f_1 and f_2 are actual (positive) functions. Isothermal contribution of the JT subsystem can be represented as

$$(c_\beta^{JT})^T = -a_\beta^S \frac{n^{JT} F_i^2 a_0^2}{k_B T} = -\frac{A_\beta^S}{T}, \quad (4)$$

where a_0 is the distance between the JT ion and the nearest neighborhood, k_B is the Boltzmann constant, n^{JT} – concentration of JT complexes, F_i – linear constant of vibronic coupling, a_β^S – coefficient (positive) depending on symmetry properties of global minima of AP, crystal symmetry and the component of the elasticity modulus tensor. For cubic complexes in crystals with structure of fluorite expressions for $(c_\beta^{JT})^T$ are listed, in particular, in [15].

In the present work, the trigonal modulus of elasticity $c_T = c_{44}$ and longitudinal modulus $c_L = c_{11}$ were investigated. These moduli are associated with normal modes propagating along the crystallographic axis [100]: transverse and longitudinal. The temperature dependences of the real and imaginary components of these moduli show anomalies typical of the JTE manifestation. An example of such dependences is shown in Fig. 3.

3. RELAXATION TIME

The configurational relaxation time τ can be calculated using data on the temperature dependences of the real part of the JT contribution $\text{Re} c_\beta^{JT}$ to the dynamic modulus of elasticity [20]:

$$\tau = \frac{1}{\omega} \sqrt{2 \frac{\text{Re} [c_\beta^{JT}(T_1) / c_0] T_1}{\text{Re} [c_\beta^{JT}(T) / c_0] T} - 1}, \quad (5)$$

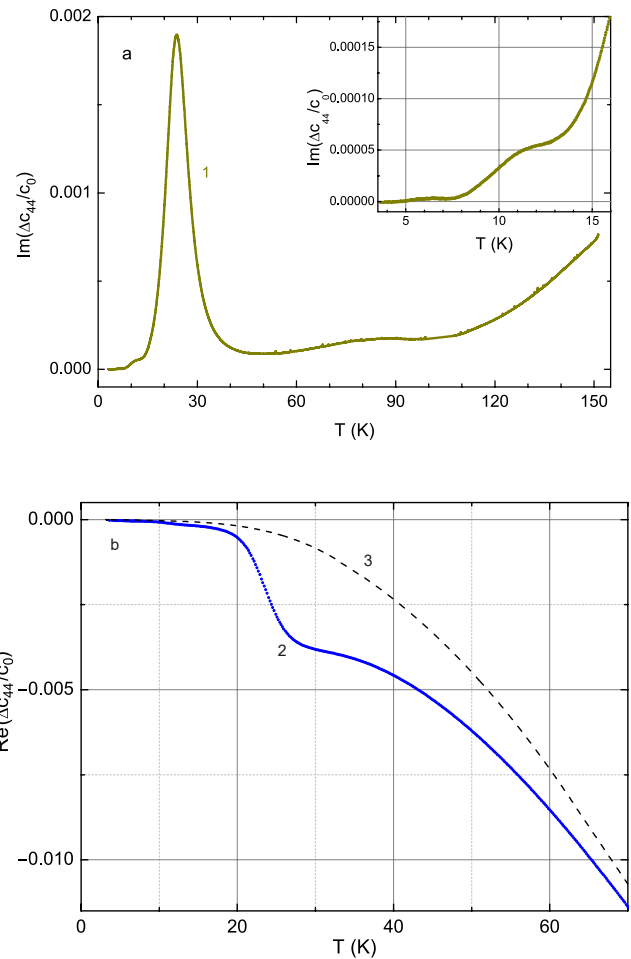


Fig. 3. Temperature dependences of the imaginary (a) and real (b) components of the elastic modulus c_{44} . Curves 1 and 2 are measured at $\omega/2\pi = 56.16$ MHz in the crystal $\text{CdF}_2 : \text{Cr}^2$. Curve 3 is the real

component of the same module in nominally pure CdF_2 measured at 56.43 MHz. $\Delta c_{44} = c_{44}(T) - c_0$, $c_0 = c_{44}(T_0)$, $T_0 = 4.2$ K. The inset shows the low-temperature part of the curve 1.

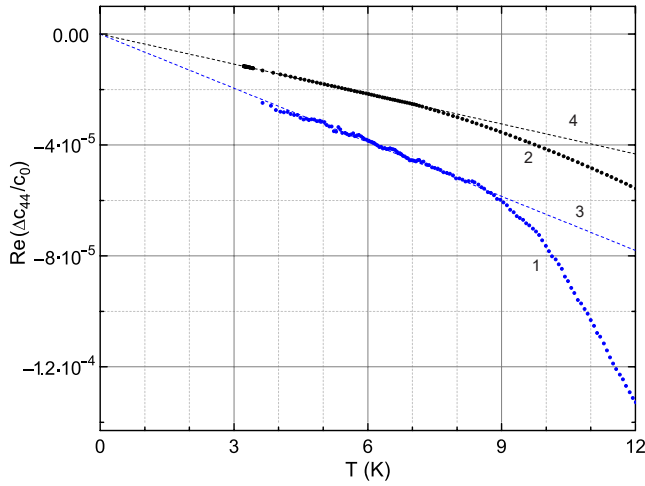


Fig. 4. Temperature dependences of the real components of the elastic modulus c_{44} in $\text{CdF}_2 : \text{Cr}$ (curve 1) and CdF_2 (curve 2) crystals; 3 and 4 – linear asymptotes. $\Delta c_{44} = c_{44}(T) - c_0$, $c_0 = c_{44}(T \rightarrow 0)$.

where

$$\text{Re} \left[\frac{c_{\beta}^{JT}(T)}{c_0} \right] = \text{Re} \left[\frac{c_{\beta}(T)}{c_0} \right] - \text{Re} \left[\frac{c_{\beta}^b(T)}{c_0} \right]$$

is the difference between the temperature dependences obtained on impurity and nominally pure crystals (curves 1 and 2 in Fig. 4, respectively), and T_1 satisfies the condition $\omega\tau = 1$. A detailed description of the method of constructing the temperature

dependence of the relaxation time is given in Sect. 4.2 in [14]. Further, under the assumption that relaxation is determined by three mechanisms (activation, tunneling, and two-phonon) [9], the parameters determining them were established by means of modeling. The results of the calculations are shown in Fig. 5, where curve 2 represents the total relaxation time $\tau = (\tau_a^{-1} + \tau_t^{-1} + \tau_R^{-1})^{-1}$, and the relaxation rates characterizing the individual mechanisms have the following form

$$\tau_a^{-1} = \tau_0^{-1} \exp \left(-\frac{V_0}{k_B T} \right), \quad (6)$$

$$\tau_t^{-1} = BT, \quad (7)$$

$$\tau_R^{-1} = \frac{B}{\Theta^2} T^3, \quad (8)$$

where V_0 is the activation energy, τ_0^{-1} is the frequency of attempts. In this form, the constants B and B/Θ^2 were introduced in [21], although originally [22] they related the relaxation time, not the rate, to the temperature in the appropriate degree. From Fig. 5 we can see that the model curve 2 generally agrees well with the experimental data, except for the region $1/T = 0.06-0.10 \text{ K}^{-1}$, where other JT subsystems are manifested, discussed below.

4. DISCUSSION

Anomalies similar to those depicted in Fig. 3, were also observed for the c_{11} module. In appearance, they are typical for JTE in impurity crystals, and the fact that they appear in the modules c_{44} and c_{11} indicates that the global minima of AP have orthorhombic

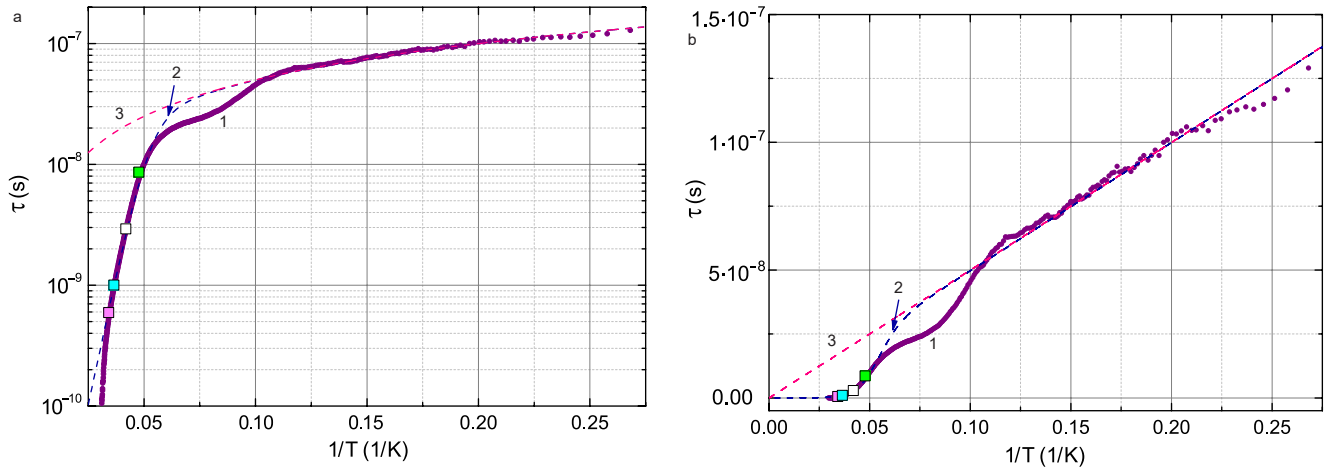


Fig. 5. Dependences of the configurational relaxation time of the JT subsystem on the inverse temperature in semi-logarithmic (a) and linear (b) coordinates. Curve 1 is plotted using the data $\text{Re} \Delta c_{44}(T)/c_0$, 2 is the model curve, curve 3 is the relaxation time due to the tunneling mechanism, $\tau_t = 1.5 \cdot 10^{-6} / T$ c. The square symbols correspond to the condition $\omega\tau = 1$ for 268, 159, 56.2, 18.3 MHz (from left to right).

symmetry. The procedure for determining the symmetry properties of the AP extrema is described in detail in [15]. In addition, it should be noted that in Fig. 3, in addition to the main features at $T \approx 25$ K (a peak on the temperature dependence of the imaginary part of the modulus and a blurred step on the graph of the real part), there are weak contributions at $T \approx 6$ K and $T \approx 11$ K, clearly visible in the inset to Fig. 3a. We assume that it is the manifestation of JT subsystems formed by Mn^{3+} or V^{2+} ions. The dope concentrations of manganese and vanadium were $(1.38 \pm 0.03) \cdot 10^{18} \text{ cm}^{-3}$ and $(1.49 \pm 0.03) \cdot 10^{18} \text{ cm}^{-3}$, respectively. Although the manifestation of JTE due to Ni^{2+} or Cu^{2+} ions also cannot be excluded due to the sensitivity of the method even to small impurity concentrations.

Temperature dependences of the imaginary part of the dynamic modulus (or ultrasound absorption) at known concentration of JT complexes n^{JT} allow us to calculate linear vibronic constants. In particular, the trigonal linear vibronic coupling constant F_T is determined from the data $\alpha_{44}^{JT}(T)$ (see, e.g., [13]) or $\text{Im}c_{44}^{JT}(T)$ (taking into account relation (2)):

$$F_T^2 = 9 \frac{c_0 k_B T_1}{n^{JT} a_0^2} \frac{\alpha_{44}^{JT}(T_1)}{k_0} = \frac{9 c_0 k_B T_1}{2 n^{JT} a_0^2} \frac{\text{Im}c_{44}^{JT}(T_1)}{c_0}. \quad (9)$$

The calculation performed according to formula (9) under the assumption $n^{JT} = n_{\text{Cr}}$, resulted in a value of $|F_T| = 1.4 \cdot 10^{-5} \text{ dyn}$ in the $\text{CdF}_2 : \text{Cr}$ crystal. This is certainly an estimate from below, but appears to be a severe underestimation. First, the value obtained is smaller than all values of vibronic constants determined previously for crystals with fluorite structure by physical acoustic methods (see Table 7 in [15]). For example, in CaF_2 and SrF_2 , also doped with chromium ions, the trigonal linear vibronic coupling constant is $8.8 \cdot 10^{-5}$ and $5.5 \cdot 10^{-5}$, respectively. Secondly, the optical spectra, [6] obtained on crystals similar to the one we used, were interpreted under the assumption of the predominance of Cr^{3+} ions, which are displaced from the central position, falling into the octahedral environment [23, 24]. They do not possess a basic orbital-excited state and thus do not form JT complexes. We suppose that in the CdF_2 crystal with chromium admixture studied by us, most of the chromium ions have the charge state $3+$ and only a smaller part of the ions isovalently substitutes for the cation, forming an JT-complex $\text{Cr}^{2+}\text{F}_8^-$. To estimate the concentration of such centers in CdF_2 , one can compare the absorption level in this crystal with the absorption in $\text{CaF}_2:\text{Cr}$ [25], which was almost 30 times smaller. It is known that

the relaxation absorption is proportional to the concentration of JT centers. Thus, the ultrasonic experiment in the $\text{CdF}_2 : \text{Cr}$ crystal showed Cr^{2+} ions with a concentration of the order of 10^{18} cm^{-3} , which leads to a more realistic value of $|F_T| = 10^{-4} \text{ dyn}$. The uncertainty in the concentration of JT ions is a significant obstacle to comparing JT subsystems formed by different $3d$ ions in different matrices using data on vibronic constants, linear and quadratic. The same circumstance makes it impossible to estimate the linear and quadratic contributions to the Hamiltonian, although the presence of relaxation-type anomalies in the $\Delta c_{44}(T)$ and $\Delta c_{11}(T)$ dependences unambiguously points to the orthorhombic symmetry of the global minima of the AP, which is possible only in the presence of an appreciable quadratic contribution to the Hamiltonian of the JT complex.

This problem is absent when finding the parameters determining the relaxation time, since its calculation does not require knowledge of the concentration of JT ions. It is the data characterizing the quantum dynamics of JT subsystems that can serve as an information base for comparing JT complexes in different matrices. The values of these parameters, determined earlier and in the present work, for different fluorites with different impurities of transition elements are presented in the table. The values of temperature T_1 , near which the relaxation absorption peak is observed if measurements are made at the frequency $\omega/2\pi = 50 \text{ MHz}$, are also given there. In the low-temperature region at frequencies 10^7 Hz and higher, the condition $\omega\tau \gg 1$ is satisfied. In this case, equation (3) taking into account (4) will take the form

$$\left(\frac{c_{\beta}^{JT}}{c_0} \right)_{\omega\tau \gg 1} = -\frac{A_{\beta}^S}{c_0 T} \left(\frac{\tau^{-2}}{\omega^2} - i \frac{\tau^{-1}}{\omega} \right). \quad (10)$$

It can be seen that the contributions of the JT subsystem to the real and imaginary components of the dynamic elasticity moduli are proportional to the relaxation rates squared and to the first degree, respectively. Therefore, relaxation rates given by relations (6)-(8) are given in the table.

If we compare the parameters characterizing the relaxation of $\text{Cr}^{2+}\text{F}_8^-$ complexes in the matrices studied by us, it makes sense to give the values of the lattice constant a and the atomic mass M of the matrix cation. The former affects the size of the complex, while the latter can have an effect through the following coordination spheres: $a_{\text{CdF}_2} = 5.399 \text{ \AA}$, $a_{\text{CaF}_2} = 5.463 \text{ \AA}$, $a_{\text{SrF}_2} = 5.799 \text{ \AA}$ [28], $M_{\text{CaF}} = 40.078 \text{ g/mol}$, $M_{\text{Sr}} = 87.62 \text{ g/mol}$, $M_{\text{Cd}} = 112.41 \text{ g/mol}$. The parameter

Table. Parameters characterizing the relaxation of the subsystem of JT complexes in some crystals with fluorite structure investigated by ultrasonic methods. The value of T_1 is determined from the maximum of the function $f_2(T) = \omega\tau / [1 + (\omega\tau)^2]$ for $\omega/2\pi = 50$ MHz

Free ion config.	Matrix	Ion	Ground state	V_0 , cm^{-1}	τ_0^{-1} , c^{-1}	B , $\text{c}^{-1} \cdot \text{K}^{-1}$	B/Θ_0^2 , $\text{c}^{-1} \cdot \text{K}^{-3}$	T_1 , K	Reference
d^4	CaF_2	Cr^{2+}	${}^5T_{2g}(e_g^2 t_{2g}^2)$	91.7	$3.3 \cdot 10^{12}$	$2.8 \cdot 10^6$	$1.0 \cdot 10^5$	8.8	[25]
d^9	BaF_2	Cu^{2+}	${}^2T_{2g}(e_g^4 t_{2g}^5)$	93.8	$2.0 \cdot 10^{11}$	$1.4 \cdot 10^6$	$2.0 \cdot 10^4$	18.8	[27]
d^9	CaF_2	Cu^{2+}	${}^2T_{2g}(e_g^4 t_{2g}^5)$	118	$3.3 \cdot 10^{11}$	$1.5 \cdot 10^6$	$5.0 \cdot 10^2$	23.8	[15]
d^4	CdF_2	Cr^{2+}	${}^5T_{2g}(e_g^2 t_{2g}^2)$	139	$1.4 \cdot 10^{12}$	$6.7 \cdot 10^5$	$1.0 \cdot 10^2$	23.3	
d^4	SrF_2	Cr^{2+}	${}^5T_{2g}(e_g^2 t_{2g}^2)$	264	$1.4 \cdot 10^{12}$	$3.6 \cdot 10^4$	$2.9 \cdot 10^2$	44.4	[26]
d^8	CaF_2	Ni^{2+}	${}^3T_{1g}(e_g^4 t_{2g}^4)$	396	$1.0 \cdot 10^{13}$	$5.6 \cdot 10^5$	$6.7 \cdot 10^1$	54.3	[14]

that most characterizes the relaxation is the activation energy. It (together with the energy of zero vibrations) determines the height of the potential barrier. Relative to this parameter, the studied JT complex occupies an intermediate position in CdF_2 compared to CaF_2 and SrF_2 , while Cd is the heaviest cation and CdF_2 has the smallest lattice constant of the considered ones. Apparently, a combination of several factors (primarily those considered) determines the relaxation properties of the system of $\text{Cr}^{2+}\text{F}_8^{2-}$ complexes in different matrices.

5. CONCLUSIONS

Ultrasonic studies of CdF_2 crystal doped with low concentration chromium ions ($n_{\text{Cr}} = 6.3 \cdot 10^{19} \text{ cm}^{-3}$) have revealed anomalies of the real and imaginary components of the dynamic elasticity moduli, which are characteristic for the manifestation of JTE at iso-valent substitution of cations. It is shown that the temperature dependence of the configurational relaxation time is well described by three mechanisms: activation, tunneling, and two-phonon. The parameters characterizing the relaxation rate for these mechanisms have been determined. Comparison of the parameters of relaxation rates in the crystal studied in the present work with similar parameters in $\text{CaF}_2 : \text{Cr}^{2+}$ and $\text{SrF}_2 : \text{Cr}^{2+}$ has shown that in $\text{CdF}_2 : \text{Cr}$ they have intermediate values and an increase in the mass of the matrix cation does not lead to a monotonic increase in the activation energy and low-temperature relaxation time.

FUNDING

This work was financially supported by the Russian Science Foundation (project No. 22-22-00735).

REFERENCES

1. R. C. Powell, *Symmetry, Group Theory, and the Physical Properties of Crystals*, Springer, New York, Dordrecht, Heidelberg, London, (2010).
2. G. Boulon, *Opt. Mater.* **34**, 499 (2012).
3. N.M. Avram and M.G. Brik (Editors), *Optical Properties of 3d-Ions in Crystals: Spectroscopy and Crystal Field Analysis*, Springer, Heidelberg, New York, Dordrecht, London (2013).
4. R. Alcalá, P. J. Alonso, V. Orera, H V. den Hartog, *Phys. Rev. B* **32**, 4158 (1985).
5. M. M. Zaripov, V. F. Tarasov, V. A. Ulanov, G. S. Shakurov, *Physics of the Solid State* **44**, 2050 (2002).
6. A.V. Egranov, E. A. Radzhabov, V. A. Kozlovsky, *Bulletin of the Russian Academy of Sciences: Physics*, **86** (7), 802 (2022).
7. J. T. Vallin, G. A. Slack, S. Roberts, A E. Hughes, *Phys. Rev. B* **2**, 4313 (1970).
8. I. B. Bersuker, V. Z. Polinger, *Vibroniv Interactions in Molecules and Crystals*, Springer- Verlag, Berlin, Heidelberg, New York, London, (1989).
9. M. D. Sturge, The Jahn Teller Effect in Solids, in: F. Seitz, D. Turnbull, H. Ehrenreich (Eds.), *Solid State Physics, Academic Press*, **20**, 91 (1967).
10. N. E. Sluchanko, E. S. Zhukova, L. N. Alyabyeva, B. P. Gorshunov, A. V. Muratov, Yu. A. Aleshchenko, A. N. Azarevich, M. A. Anisimov, N. Yu.

- Shitsevalova, S. E. Polovets and V. B. Filipov, *JETP* **136**, 148 (2023).
11. A. V. Sobolev, V. I. Nitsenko, A. A. Belik, I. S. Glazkova, M. S. Kondratyeva and I. A. Presniakov, *JETP* **137**, 404 (2023).
 12. I. V. Zhevstovskikh, I. B. Bersuker, V. V. Gudkov, N. S. Averkiev, M. N. Sarychev, S. Zherlitsyn, S. Yasin, G. S. Shakurov, V. A. Ulanov, and V. T. Surikov, *J. Appl. Phys.* **119**, 225108 (2016).
 13. M. N. Sarychev, W. A. L. Hosseny, A. S. Bondarevskaya, I. V. Zhevstovskikh, A. V. Egranov, O. S. Grunskiy, V. T. Surikov, N. S. Averkiev, V. V. Gudkov, *J. Alloy. Comp.* **848**, 156167 (2020).
 14. M. N. Sarychev, A. S. Bondarevskaya, I. V. Zhevstovskikh, V. A. Ulanov, G. S. Shakurov, A. V. Egranov, V. T. Surikov, N. S. Averkiev, V. V. Gudkov, *JETP* **132**, 790 (2021).
 15. M. N. Sarychev, W. A. L. Hosseny, I. V. Zhevstovskikh, V. A. Ulanov, A. V. Egranov, V. T. Surikov, N. S. Averkiev, V. V. Gudkov, *JETP* **135**, 473 (2022).
 16. I. B. Bersuker, *The Jahn-Teller Effect*, Cambridge University Press, Cambridge, (2006).
 17. M. M. Zaripov, V. F. Tarasov, V. A. Ulanov, G. S. Shakurov, M. L. Popov, *Sov. Phys. — Fizika Tverdogo Tela* **37**, 806 (2006).
 18. V. A. Ulanov, M. M. Zaripov, E. P. Zheglov, R. M. Ermina, *Physics of the Solid State* **45**, 73 (2003).
 19. M. N. Sarychev, *Investigation of the dynamics of Jahn-Teller complexes in crystals by methods of physical acoustics, diss. cand. of phys.-math. sciences*, UrFU, Ekaterinburg (2023).
 20. V. V. Gudkov, Ultrasonic consequences of the Jahn Teller effect, in: H. Koppel, D. R. Yarkony, H. Barentzen (Eds.), *The Jahn Teller Effect: Fundamentals and Implications for Physics and Chemistry*, Springer, Berlin, Heidelberg, **743** (2009).
 21. M. D. Sturge, J. T. Krause, E. M Gyorgy, R. C. LeCraw, F. R. Merritt, *Phys. Rev.* **155**, 218 (1967).
 22. R. Pirc, B. Zeks, P. Gosar, *J. Phys. Chem. Solids* **27**, 1219 (1966).
 23. S. A. Payne, L. L. Chase, W. F. Kupke, *J. Chem. Phys.* **86**, 3455 (1987).
 24. S. A. Payne, L. L. Chase, W. F. Kupke, *J. Lumin.* **40**, 305 (1988).
 25. M. N. Sarychev, W. A. L. Hosseny, I. V. Zhevstovskikh, V. A. Ulanov, G. S. Shakurov, A. V. Egranov, V. T. Surikov, N. S. Averkiev, V. V. Gudkov, *J. Phys.: Condens. Matter* **34**, 225401 (2022).
 26. M. N. Sarychev, W. A. L. Hosseny, A. S. Bondarevskaya, G. S. Shakurov, V. A. Ulanov, V. T. Surikov, I. V. Zhevstovskikh, N. S. Averkiev, V. V. Gudkov, *AIP Conference Proceedings* **2313**, 030071 (2020).
 27. N. Yu. Ofitserova, M. N. Sarychev, I. V. Zhevstovskikh, V. A. Ulanov, V. T. Surikov, N. S. Averkiev, V. V. Gudkov, *J. Phys.: Conf. Ser.* (accepted for publication).
 28. W. Gehlhoff, W. Ulrici, *Phys. Stat. Sol. B* **102**, 11 (1980).